IOPscience iopscience.iop.org

Home Search Collections Journals About Contact us My IOPscience

Simulation study on the first penetration field in type-II superconductors

This article has been downloaded from IOPscience. Please scroll down to see the full text article.

1997 J. Phys.: Condens. Matter 9 10203

(http://iopscience.iop.org/0953-8984/9/46/018)

View the table of contents for this issue, or go to the journal homepage for more

Download details:
IP Address: 171.66.16.209
The article was downloaded on 14/05/2010 at 11:06

Please note that terms and conditions apply.

J. Phys.: Condens. Matter **9** (1997) 10203–10209. Printed in the UK PII: S0953-8984(97)82106-6

Simulation study on the first penetration field in type-II superconductors

Yoshihisa Enomoto† and Kazuma Okada‡

† Department of Physics, Nagoya Institute of Technology, Gokiso, Nagoya 466, Japan
‡ Department of Applied Physics, Nagoya University, Nagoya 464-01, Japan

Received 24 February 1997, in final form 22 August 1997

Abstract. On the basis of computer simulations of the time-dependent Ginzburg–Landau model including thermal noise effects, we evaluate the surface barrier against magnetic flux penetration in type-II superconductors. We discuss several parameter dependencies of the first field for flux penetration, which is estimated from the first peak position of the magnetization curve in the presence of an external field slowly increasing over time. It is shown that the first penetration field is a decreasing function of temperature and of the degree of sample shape deformation. The surface barrier is also found to be suppressed by the surface irregularity on the scale of the magnetic penetration depth.

It has been recognized that to gain insight into the magnetic properties of type-II superconductors, such as the magnetic flux dynamics phenomena, hysteretic magnetic response, and critical current, an intensive understanding of the surface barrier is indispensable [1]. The surface barrier arises as a result of the competition between the attractive force between a vortex inside the superconductor and its image outside, and the repulsion between the vortex and the surface shielding current [2, 3]. In order to enable flux to penetrate into a superconductor, the shielding current should be strong enough to pull the flux away from its mirror image over a distance of the order of the coherence length. This condition yields the first field for flux penetration, denoted by H_p, which exceeds the lower critical field, H_{c1}. For a perfect surface one gets $H_p \simeq H_c$ where H_c is the thermodynamic field [2, 3]. On the other hand, in real samples the barrier is diminished by various causes, and thus H_p lies somewhere in between: $H_{c1} < H_p < H_c$ [1].

Recently, the properties of the irreversible state of high-T_c superconductors have been found to be strongly influenced by the surface barrier. Indeed, Konczykowski *et al* [4] have demonstrated the dominant role of the surface barrier in the formation of the magnetization properties of clean untwinned YBCO crystals at high temperatures. Other evidence for the role of the surface barrier has been reported, including the observation of a crossover, which separates the bulk and the surface barrier regimes for the magnetic relaxation rate [5]. Moreover, Zeldov *et al* [6] have pointed out that the irreversible magnetic behaviour at intermediate temperatures in Bi-based compounds is determined by the surface barrier, whereas the low-temperature behaviour is due to the bulk pinning and the high-temperature behaviour is due to the geometrical barrier induced by the demagnetization effect.

Surface barrier effects have been discussed so far by using the Bean–Livingston (BL) model [2] and also extended BL models such as the Clem model [7], which are at a rather

0953-8984/97/4610203+07$19.50 © 1997 IOP Publishing Ltd

phenomenological level. In this paper, to complement the previous study, we evaluate the surface barrier by using a different type of approach, namely the numerical approach of the time-dependent Ginzburg–Landau (TDGL) equations [8, 9]. Here, simulating the TDGL model with thermal noise effects, we examine the magnetic response of type-II superconductors to a linearly increasing external magnetic field with time, and then estimate the first field, H_p, for flux penetration. In particular, we discuss several parameter dependencies of H_p, such as those on the temperature, the aspect ratio of the sample shape, and the surface irregularity.

The TDGL equations with thermal noise effects used in the simulation are as follows [8–10]:

$$\Gamma_\psi^{-1}\frac{\partial\psi}{\partial t} = -\frac{\delta F}{\delta\psi^*} + g(\boldsymbol{r},t) \tag{1}$$

$$\Gamma_A^{-1}\frac{\partial\boldsymbol{A}}{\partial t} = -\frac{\delta F}{\delta\boldsymbol{A}} + \boldsymbol{f}(\boldsymbol{r},t) \tag{2}$$

with kinetic coefficients $\Gamma_\psi = 2mD/\hbar^2$ and $\Gamma_A = c^2/\sigma$, and the Helmholtz free energy F defined by

$$F = \int \mathrm{d}\boldsymbol{r}\left[\frac{1}{2m}|\mathbf{D}\psi|^2 + \alpha(T)|\psi|^2 + \frac{\beta}{2}|\psi|^4 + \frac{1}{8\pi}(\boldsymbol{\nabla}\times\boldsymbol{A})^2\right] \tag{3}$$

where $\mathbf{D} \equiv -\mathrm{i}\hbar\boldsymbol{\nabla} - (e/c)\boldsymbol{A}$ is the covariant derivative. Here, $\psi(\boldsymbol{r},t)$ is the complex order parameter at time t and position $\boldsymbol{r}$, and $\boldsymbol{A}(\boldsymbol{r},t)$ is the vector potential with the local magnetic flux density $\boldsymbol{b}(\boldsymbol{r},t) \equiv \boldsymbol{\nabla}\times\boldsymbol{A}$. The other symbols have their usual meanings [11]. We work in the zero-scalar-potential gauge [8, 9]. The last terms of the r.h.s. of equations (1) and (2), g and $\boldsymbol{f}$, denote the thermal noise effects. These noise terms are characterized [12] by $\langle\langle g\rangle\rangle = \langle\langle \boldsymbol{f}\rangle\rangle = 0$, and

$$\langle\langle g^*(\boldsymbol{r}',t')g(\boldsymbol{r},t)\rangle\rangle = 2\Gamma_\psi^{-1}k_BT\delta(\boldsymbol{r}'-\boldsymbol{r})\delta(t'-t) \tag{4}$$

$$\langle\langle f_i(\boldsymbol{r}',t')f_j(\boldsymbol{r},t)\rangle\rangle = 2\Gamma_A^{-1}k_BT\delta(\boldsymbol{r}'-\boldsymbol{r})\delta(t'-t)\delta_{ij} \tag{5}$$

with all cross correlations being zero, where $\langle\langle\cdots\rangle\rangle$ denotes an average with respect to the noise distribution, and f_i is the ith component of $\boldsymbol{f}$. Under the assumption that $\alpha(T) = \alpha(0)(T/T_c - 1)$ with two positive constants $\alpha(0)$ and β in equation (3), the coherence length and the magnetic penetration depth are given by $\xi(T) = \xi(0)(1-T/T_c)^{-1/2}$ and $\lambda(T) = \lambda(0)(1-T/T_c)^{-1/2}$, respectively, with the critical temperature T_c at zero field. We also obtain three critical fields in units of $H_{c2}(0)$: $H_{c2}(T)/H_{c2}(0) = 1 - T/T_c$, $H_{c1}(T)/H_{c2}(0) = (\ln\kappa/(2\kappa^2))(1-T/T_c)$, and $H_c(T)/H_{c2}(0) = ((1/(\sqrt{2}\kappa))(1-T/T_c)$ with the GL parameter $\kappa \equiv \lambda(T)/\xi(T) = \lambda(0)/\xi(0)$.

We here consider a superconducting rectangular sample which is assumed to be infinite in the z-direction with a cross sectional area $L_x \times L_y$ in the x–y plane. The external magnetic field, $H_e(t)$, is applied to the system in the z-direction, and is slowly changing with time t as $H_e(t) = \gamma(t/t_0)H_{c2}(T)$ with the variation rate γ and $t_0 \equiv \pi\hbar/(96k_BT_c)$. Moreover, neglecting all derivatives along the z-axis and also the demagnetization effects, we reduce the problem to two dimensions. The present results, therefore, apply only to bulk materials where fluctuations in the z-direction have been neglected.

In actual simulations the TDGL equations are transformed into the dimensionless discretized equations on a two-dimensional lattice by introducing link variables for the vector potential. In contrast with previous work [8, 9], we use here temperature-dependent system sizes (for most cases, $L_x = L_y = 256\,\xi(T)$) to include the thermal effects effectively, since the flux penetration processes are strongly affected by these effects. In

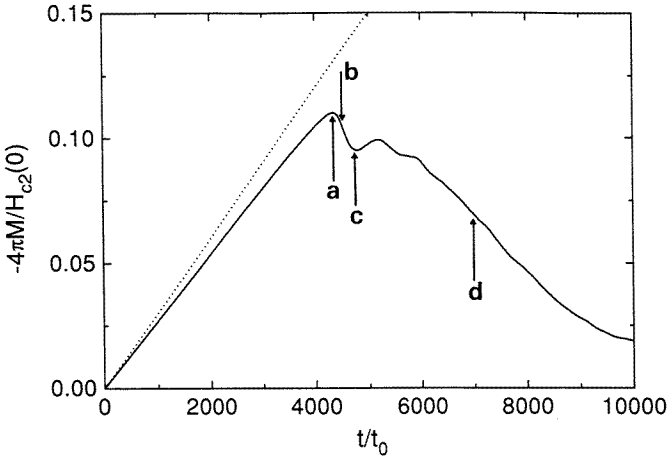

Figure 1. The time variation of the magnetization $M(t)$ for $L_x = L_y = 256\,\xi(T)$ at $T/T_c = 0.7$, shown by a solid line. The dotted line denotes the external field $H_e(t)$ in units of $H_{c2}(0)$. Labels a–d with arrows correspond to the panels of figure 2.

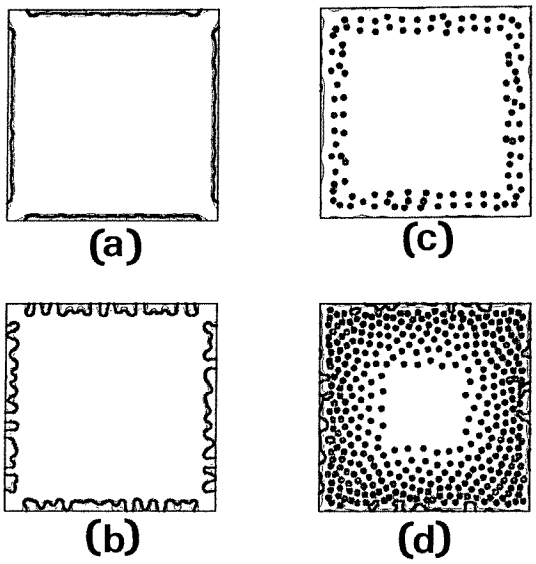

Figure 2. The time variation of the contour line of the order parameter amplitude $|\psi(\boldsymbol{r}, t)|$ at $t/t_0 = 4350$ (a), 4500 (b), 4700 (c), and 7000 (d) for the same parameter values as in figure 1.

the following simulations, we set $\kappa = 4$, and also take the lattice spacing and time step for numerical calculations to be $0.5\,\xi(T)$ and $0.0125\,t_0$, respectively. These values are chosen for computational reasons, to obtain results efficiently within our computer availability. As the initial state, we choose the zero-field-cooling state. Details of the computational method can be found in our previous work [8, 9].

Firstly, we examine the process of penetration of the magnetic flux and/or vortices into the sample, which is in a superconducting state in the absence of the external field at $t = 0$. In figure 1 we show the time variation of the magnetization, $M(t)$, for $L_x = L_y = 256\,\xi(T)$

at $T = 0.7\,T_c$ and $\gamma = 10^{-4}$, where the dotted line denotes the time-dependent external field $H_e(t)$. The magnetization $M(t)$ is defined as $4\pi M(t) = \langle B\rangle(t) - H_e(t)$, where the magnetic induction $\langle B\rangle(t)$ is obtained from the sample average of the z-component, $b_z(\boldsymbol{r}, t)$, of the local magnetic flux density $\boldsymbol{b}(\boldsymbol{r}, t)$. The resulting curve, $-4\pi M(t)$, exhibits a few maxima, which are not sharp for large values of $H_e(t)$. In figure 2 we show the corresponding time variation of contour lines of the order parameter amplitude $|\psi(\boldsymbol{r}, t)|$. Calculating the magnetic flux, we have confirmed that each definite circular pattern appearing in these figures corresponds to a quantized magnetic vortex with one flux quantum [9]. From these results we can see that the magnetic flux first penetrates into the superconducting sample from the sample boundaries to form walls (figure 2(a)), and then the walls become irregular (figure 2(b)) to break up into vortices (figure 2(c)), following the increase of the applied field [9]. For further higher fields, irregular penetrating flux regions near the sample boundaries continuously emerge and are the sources of vortex creations (figure 2(d)), and simultaneously vortices diffuse towards the centre of the sample [9]. We have checked that after each maximum of the $-4\pi M(t)$ curve shown in figure 1 a sudden creation of magnetic vortices from the irregular flux boundaries takes place. Similar behaviour has been obtained by Bolech *et al* [13]. In the following discussion, the first penetration field $H_p(T)$ is calculated from the first bending point of $M(t)$.

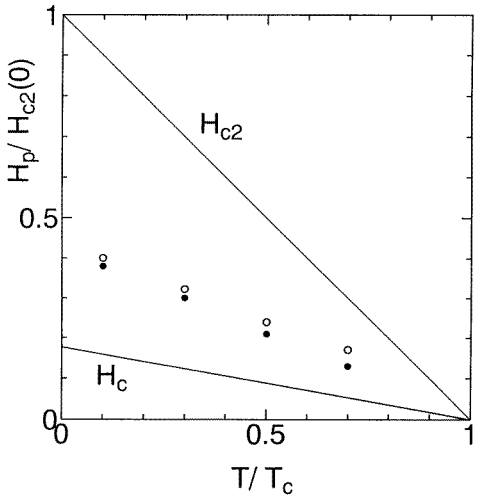

Figure 3. The temperature dependence of the first penetration field $H_p(T)$ for $L_x = L_y = 256\,\xi(T)$ with (●) and without (○) thermal noise effects. The upper critical field $H_{c2}(T)$ and the thermodynamic critical field $H_c(T)$ are also shown for comparison, in units of $H_{c2}(0)$.

Secondly, we study the temperature dependence of the surface barrier. In figure 3 we show the first penetration field $H_p(T)$ as a function of temperature T for $L_x = L_y = 256\,\xi(T)$ and $\gamma = 10^{-4}$. In this figure, for comparison, we also plot $H_p(T)$ for the case without thermal noise effects. It is shown that $H_p(T)$ is a decreasing function of T, as was discussed in many previous studies [1–3], and also thermal noise effects enhance the flux penetration and thus lower H_p. Similar behaviour has been obtained for the case of $\gamma = 10^{-5}$. We should remark that in the present simulations we obtain $H_p(T) > H_c(T)$, in contrast with the previous result, $H_p(T) \leqslant H_c(T)$ [1–3]. A plausible reason for this discrepancy might be the finiteness of our simulation systems. In fact, we have obtained $H_p(T)/H_c(T) = 2.45$ for $L_x = L_y = 256\,\xi(T)$, 2.11 for $512\,\xi(T)$, and 1.53 for $768\,\xi(T)$ at

$T/T_c = 0.7$ with thermal noise effects. These results indicate that $H_p(T)$ tends to decrease with increasing system size. To confirm this, further detailed simulations with changed parameter values are needed and are now under way.

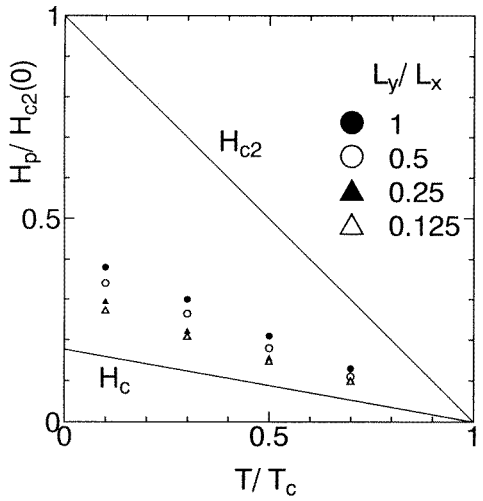

Figure 4. The dependence on the aspect ratio, $R \equiv L_y/L_x$, of the first penetration field $H_p(T)$ with $L_x = 256\,\xi(T)$ being fixed. The upper critical field $H_{c2}(T)$ and the thermodynamic critical field $H_c(T)$ are also shown for comparison, in units of $H_{c2}(0)$.

Next, we study the effect of the aspect ratio, $R \equiv L_y/L_x$, on the surface barrier. In figure 4 we show the first penetration field $H_p(T)$ as a function of temperature T at $\gamma = 10^{-4}$ for $R = 1$, 0.5, 0.25, and 0.125, with $L_x = 256\,\xi(T)$ being fixed. A small aspect ratio corresponds to a substantial degree of deformation of the sample shape. From these results, $H_p(T)$ is found to be a decreasing function of the degree of sample shape deformation. This behaviour is thought to be due to the collective interaction among nearby magnetic fields. Moreover, we examine how the results change with the system size. We have determined the ratio of H_p for $R = 0.25$ to H_p for $R = 1$ to be 0.746 for $L_x = 256\,\xi(T)$, 0.817 for $512\,\xi(T)$, and 0.905 for $768\,\xi(T)$ at $T/T_c = 0.7$. These results might indicate that the effects of the aspect ratio on the surface barrier become less important with increasing system size. However, these effects on the surface barrier have been less studied so far. Further study is needed experimentally, theoretically, and computationally.

Finally, we study the effect of the surface irregularity on the surface barrier. The surface irregularity is modelled as a surface defect, and is introduced such that the coefficient α in the GL free energy (3) is set to be zero at the defect's position. Here, 40 defects with the size $\lambda(T) \times \lambda(T)$ are randomly distributed on the sample boundaries for each value of temperature, as is shown in figure 5. In figure 6 we show the first penetration field $H_p(T)$ as a function of temperature T for $L_x = L_y = 256\,\xi(T)$ and $\gamma = 10^{-4}$ with and without surface defects. We have checked that surface defects with the size $\xi(T) \times \xi(T)$ have no evident effects on $H_p(T)$. The surface irregularity on the scale of $\lambda(T)$ is thought to result in new gates for the flux penetration and thus to weaken the surface barrier. These results are in qualitative agreement with recent experimental data on high-T_c superconductors [4].

In conclusion, we have demonstrated several parameter dependencies of the surface barrier against magnetic flux penetration on the basis of numerical calculation of the TDGL equations with thermal noise effects. We have shown that the first penetration field $H_p(T)$

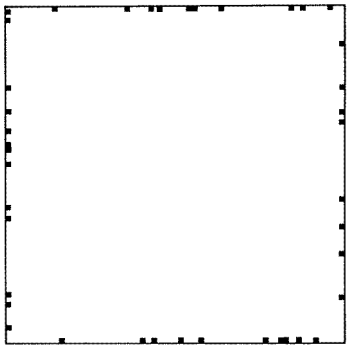

Figure 5. Defects randomly distributed on the sample boundaries, denoted by black squares with the size $\lambda(T) \times \lambda(T)$ for the $256\,\xi(T) \times 256\,\xi(T)$ system.

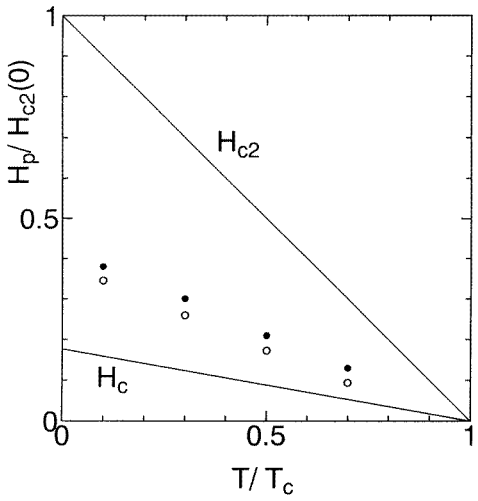

Figure 6. The first penetration field $H_p(T)$ for $L_x = L_y = 256\,\xi(T)$ with (○) and without (●) surface defects. The upper critical field $H_{c2}(T)$ and the thermodynamic critical field $H_c(T)$ are also shown for comparison, in units of $H_{c2}(0)$.

is a decreasing function of both temperature and the degree of sample shape deformation. The thermal noise effect is also shown to enhance the flux penetration. Moreover, surface irregularities on the scale of $\lambda(T)$ have been found to suppress the surface barrier and then to lower $H_p(T)$, while surface defects on the scale of $\xi(T)$ have no evident effects on $H_p(T)$ in the present simulations. The effects of the system size on these results have also been studied a little. However, this study is at a primitive stage and thus the detailed discussion of the problem will be presented elsewhere.

Here, we have restricted the present simulations to a study of the effect of the surface barrier on the magnetic flux penetration process, neglecting the z-dependence of the problem and also the demagnetization effect. Recent experiments and theoretical analyses have revealed that the magnetic properties of high-T_c materials are affected by various features [1], such as bulk pinning [4, 5], the geometrical barrier due to the demagnetization effect [6], the bending of flux lines, and quantum tunnelling of point-like vortices [14]. Moreover,

the asymmetry exhibited by the surface barrier between the flux entry and the flux exit processes in the presence of a transport current has been pointed out [15]. The results obtained here cannot be directly applied to these cases. However, the present study might give a useful guide for discussion of the magnetic properties in such complicated situations. These effects, as well as study of the magnetic hysteresis loop, will be discussed in future work.

Acknowledgments

The authors are grateful to Professor S Maekawa and Dr N Wilkin for a number of valuable comments.

References

[1] For a review, see
Brandt E H 1995 *Rep. Prog. Phys.* **58** 1465
Yeshurun Y, Malozemoff A P and Shaulov A 1996 *Rev. Mod. Phys.* **68** 911
[2] Bean C P and Livingston J D 1964 *Phys. Rev. Lett.* **12** 14
[3] de Gennes P-G 1966 *Superconductivity of Metals and Alloys* (New York: Benjamin)
[4] Konczykowski M, Burlachkov L I, Yeshurun Y and Holtzberg F 1991 *Phys. Rev.* B **43** 13 707
[5] Chikumoto N, Konczykowski M, Motohira N and Malozemoff A P 1992 *Phys. Rev. Lett.* **69** 1260
[6] Zeldov E, Majer D, Konczykowski M, Larkin A I, Vinokur V M, Geshkenbein V B, Chikumoto N and Shtrikman H 1995 *Europhys. Lett.* **30** 367
[7] Clem J R 1974 *Proc. 13th Conf. on Low Temperature Physics* vol 3 (New York: Plenum) p 102
[8] Fram H, Ullah S and Dorsey A T 1991 *Phys. Rev. Lett.* **66** 3067
Liu F, Mondello M and Goldenfeld N 1991 *Phys. Rev. Lett.* **66** 3071
Kato R, Enomoto Y and Maekawa S 1991 *Phys. Rev.* B **44** 6916
Kato R, Enomoto Y and Maekawa S 1993 *Phys. Rev.* B **47** 8016
[9] For a review, see
Enomoto Y, Kato R and Maekawa S 1993 *Studies of High Temperature Superconductors* vol 11, ed A V Narlikar (New York: Nova Science) p 309
[10] Dorsey A T 1994 *Ann. Phys.* **233** 248
[11] Tinkham M 1975 *Introduction to Superconductivity* (New York: MacGraw-Hill)
[12] Hohenberg P C and Halperin B I 1977 *Rev. Mod. Phys.* **49** 435
[13] Bolech C, Buscaglia G C and Lopez A 1995 *Phys. Rev.* B **52** R15 719
[14] Mints R G and Shapiro I B 1993 *Phys. Rev.* B **47** 3273
[15] Burlachkov L, Koshelev A E and Vinokur V M 1996 *Phys. Rev.* B **54** 6750